ELSEVIER

Polymer 44 (2003) 2519–2527

polymer

www.elsevier.com/locate/polymer

Optical, dielectric and thermal properties of nanoscaled films of polyalkylsilsesquioxane composites with star-shaped poly(ε-caprolactone) and their derived nanoporous analogues

W. Oh[a], Y. Hwang[a], Y.H. Park[a], M. Ree[a,*], S.-H. Chu[b], K. Char[b], J.K. Lee[c], S.Y. Kim[d]

[a]*Department of Chemistry, Center for Integrated Molecular Systems, BK-21 Program, Division of Molecular and Life Sciences, and Polymer Research Institute, Pohang University of Science and Technology, San 31, Hyoja-dong, Pohang 790-784, South Korea*

[b]*School of Chemical Engineering and BK21 Program, Seoul National University, San 56-1, Shillim-dong, Kwanak-gu, Seoul 151-742, South Korea*

[c]*School of Chemistry and BK21 Program, Seoul National University, San 56-1, Shillim-dong, Kwanak-gu, Seoul 151-742, South Korea*

[d]*Department of Chemistry, Center for Advanced Functional Polymers, and School of Molecular Science (BK21), Korea Advanced Institute of Science and Technology, 373-1, Kusung-dong, Yusung-gu, Daejeon, 305-701, South Korea*

Received 16 October 2002; accepted 21 January 2003

Abstract

Nanoscaled films of poly(methylsilsesquioxane-*co*-ethylenylsilsesquioxane) (PMSSQ–BTMSE) and polymethylsilsesquioxane (PMSSQ) were prepared from the respective soluble prepolymers, and their thermal, optical, and dielectric properties were characterized. The PMSSQ–BTMSE nanofilm containing an ethylenyl bridge comonomer unit BTMSE was found to be thermally more stable than the nanofilm of PMSSQ, a representative polyalkylsilsesquioxane. Further, in comparison to the PMSSQ film the PMSSQ–BTMSE film exhibits a larger refractive index and a larger dielectric constant but a smaller out-of-plane thermal expansion coefficient, when both prepolymers are cured under the same conditions. These characteristics of PMSSQ–BTMSE films are due to the ethylenyl bridge provided by the BTMSE comonomer unit, which promotes the formation of a tighter, more perfect network structure in cured PMSSQ–BTMSE films. Composite films were prepared by solution-blending the pore generator (referred to as the porogen), a star-shaped poly(ε-caprolactone), with the soluble prepolymers then drying the resulting solution, and the nature of their curing reactions and extent of porogen calcination were investigated. It was found that the thermal curing and calcination processes of the composite films successfully produce PMSSQ–BTMSE and PMSSQ films containing pores that are about 400 nm in diameter. It was confirmed that the presence of these generated nanopores significantly reduces the refractive indices and the dielectric constants of the dielectric films but increases their out-of-plane thermal expansivity, depending on the initial porogen loading. The porosities of the nanoporous dielectric films were estimated from the measured refractive indices. The surface topographies of these films were also investigated, giving information about the sizes of the pores generated in the films. It was also found that prior to calcination the presence of the porogen increases the refractive index and dielectric constant of the composite dielectric films because of its inherent high polarizability, and also increases the thermal expansivity of MSSQ–BTMSE composite films but very slightly decreases the thermal expansivity of MSSQ composite films. It is demonstrated that PMSSQ–BTMSE films and the related nanometer scale nanoporous films are candidates for use as low and ultra-low dielectric interlayers in the fabrication of advanced microelectronic devices.

Keywords: Nanoporous dielectric film; Porogen; Porosity

1. Introduction

Advanced microelectronic devices are designed and manufactured as multilayer structures in order to enable the compact wiring of metal conductor lines, delivering improved electronic performance [1–5]. Such advanced devices require a highly conductive metal for their wiring and an ultra-low dielectric insulating material for the interdielectric layer [6–9]. Recently, many research institutes and companies have been involved in the development of interlayer dielectrics with an ultra-low dielectric constant k and a high dielectric strength. It is likely that by 2003 low-k materials will be used in combination with copper interconnects in back-end-of-the-line processes for the fabrication of integrated circuits with a feature dimension

* Corresponding author. Tel.: +82-54-279-2120; fax: +82-54-279-3399.
E-mail address: ree@postech.edu (M. Ree).

0032-3861/03/$ - see front matter © 2003 Elsevier Science Ltd. All rights reserved.
doi:10.1016/S0032-3861(03)00129-0

of 0.13 μm [6]. The reduction of the dielectric constant of these materials to values less than 2.0 is essential for future devices, and is at present only made possible by the incorporation of nanometer-sized pores into the insulating matrices [10–12]. One promising class of candidates for a low-*k* material are the spin-on glasses, for example poly(methylsilsesquioxane) (PMSSQ) and poly(phenylsilsesquioxane) (PPSSQ) [11–15]. These glasses are characterized by inherently low dielectric constants ranging from 2.7 to 2.9, low moisture uptake, and excellent thermal stability up to 500 °C [12,16]. Further, they are known to have excellent processability for processes such as planarization, gap filling, spin-on processing, damascence processing, and chem–mech polishing [11–21]. Their dielectric constants may be further decreased by the incorporation of an organic supramolecular template as a pore generator (referred to as a *porogen*) into the silsesquioxane matrices and subsequent heating to high temperatures [12,17,18,21,22]. This process results in the thermal decomposition and volatilization of the porogen, leaving behind nanoscaled pores in the dielectric films. Star-shaped and hyperbranched macromolecules that thermally degrade below 400 °C have proven to be suitable porogens [15,18,21,22].

In addition to the low dielectric constants and easy processability of these materials, their thermal expansion coefficients are comparable to those of the metal lines employed in the integrated circuit, which is a requirement of interdielectric layer materials, because a mismatch is the major factor in producing residual stress (referred to as the *interfacial stress*) [1–5,10,23–29]. In general, a larger thermal expansion coefficient of the interdielectric layer leads to a larger thermal expansion mismatch with the metal lines, resulting in larger residual stress at all possible interfaces and, as a result, mechanical failures such as curling, bending, displacement, cracking, and delamination [1–5,10,23–29].

Lee et al. [18] recently showed that cured PMSSQ films containing a small amount of an alkylene-bridged organosilicate [e.g. bis(1,2-trimethoxysilyl)ethane, BTMSE] as a comonomer exhibit better mechanical properties than PMSSQ homopolymer films and better mixing with the star-shaped poly(ε-caprolactone) porogen. Further, we have characterized the structures of nanoporous films of nanometer thickness using the synchrotron X-ray reflection technique [21]. In the present study, we used this excellent spin-on glass material [i.e. methylsilsesquioxane-*co*-ethylenylsilsesquioxane (MSSQ–BTMSE) prepolymer] for the preparation of nanoporous films and assessed their thermal stability, thermal expansivity, optical and dielectric properties, porosity, and surface topography, using thermogravimetry (TGA), ellipsometry, and atomic force microscopy (AFM). These characterizations are compared here with those of PMSSQ and its nanoporous films.

2. Experimental

2.1. Materials

MSSQ prepolymer (GR650F™), which has a weight-average molecular weight ($\bar{M}_w$) of 10,000, was supplied by Techneglas Company (USA). This precursor has an alternating silicon–oxygen network structure with methyl pendant groups as well as hydroxy and ethoxy functional groups, as shown in Fig. 1 [13,14]. MSSQ–BTMSE prepolymer was prepared from the sol–gel reaction of tetramethoxysilane (TMOS, 90 mol%) and bis(1,2-trimethoxysilyl)ethane (BTMSE, 10 mol%) in tetrahydrofuran with an acid catalyst and some water (see Fig. 1) [18]. The copolymerized prepolymer was determined to have a number-average molecular weight ($\bar{M}_n$) of 2700 g/mol and a ($\bar{M}_w$) of 5200 g/mol. A star-shaped poly(ε-caprolactone) (PCL-4), which has a biphenyl core and four arms with hydroxyl end groups (shown in Fig. 2), was synthesized according to a procedure described in the literature [22,30,31]. The porogen was measured to have a ($\bar{M}_n$) of 4390 g/mol, a ($\bar{M}_w$) of 5180 g/mol, and a degree of polymerization (DP) of 7.3/arm. In this study, all molecular weights were measured by gel permeation chromatography calibrated with polystyrene standards.

2.2. Film preparation

Si(100) substrates were cut into pieces of approximately 45 mm × 30 mm and then cleaned with piranha solution, followed by rinsing with deionized water and drying with nitrogen blow. Each prepolymer was dissolved in methyl isobutyl ketone (MIBK), giving a solution of 20 wt%. For each precursor, a series of homogeneous solutions containing the porogen was also prepared in MIBK; the porogen content was adjusted to be 0, 5, 10 and 20 wt% with respect to the prepolymer content. Each solution was filtered using a disposable syringe equipped with a polytetrafluoroethylene (PTFE) filter of pore size 0.2 μm and subsequently deposited on the precleaned silicon substrates by spin-coating at 5000 rpm for 30 s. The deposited films were heated to 100 °C at a rate of 2.0 °C/min in vacuum and held at that temperature for 1 h. The films were further heated to 250 °C at 2.0 °C/min, cured at that temperature for 1 h, and then slowly cooled to room temperature. Some of the films cured at 250 °C were further heated to 420 °C in vacuum and held at that temperature for 1 h, followed by cooling to room temperature. All films were approximately100 nm in thickness.

2.3. Measurements

TGA measurements were carried out under a nitrogen atmosphere using a Perkin–Elmer thermogravimeter (Model TGA-7). The flow rate of nitrogen gas was 80 ml/min and the heating rate was 2.0 °C/min. Surface

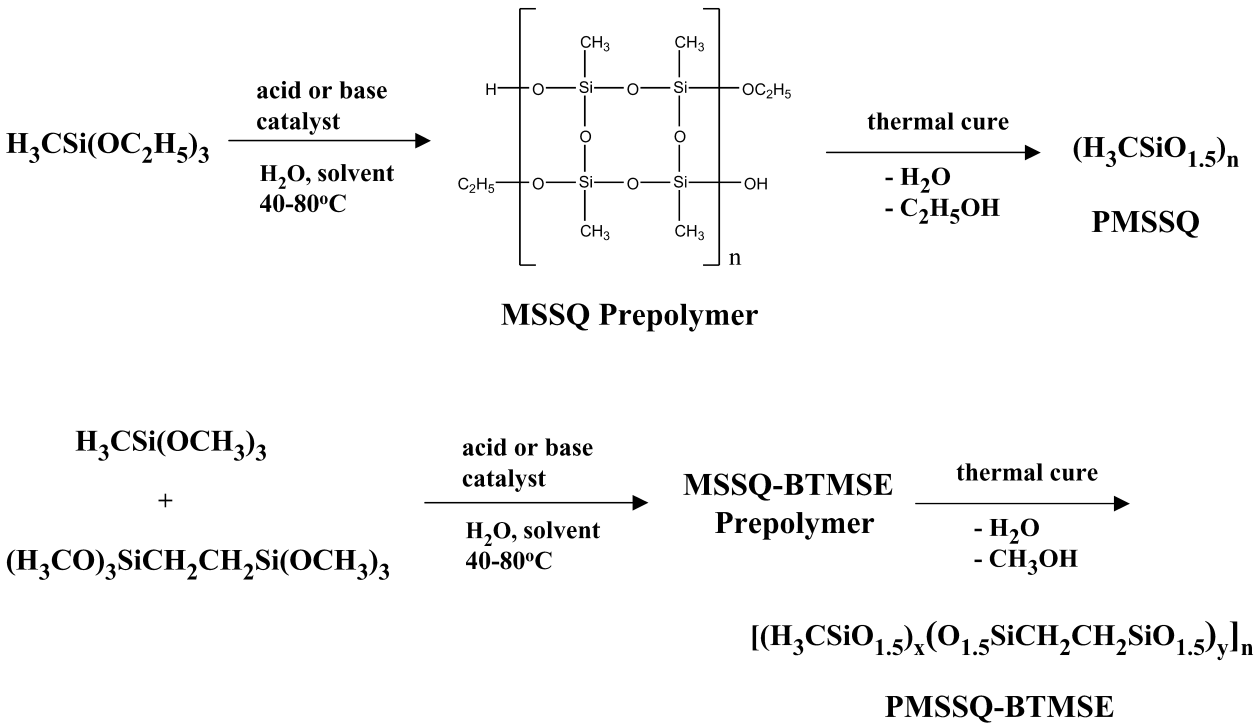

Fig. 1. Synthetic schemes of methylsilsesquioxane (MSSQ) and methylsilsesquioxane-*co*-ethylenylsilsesquioxane (MSSQ–BTMSE) prepolymers and their secondary polycondensations via thermal cure, which produce PMSSQ and PMSSQ–BTMSE as the fully cured products.

topographs were determined using an atomic force microscope (Model DME-DualScope, Danish Micro Engineering). Ellipsometry, which measures the change in the polarization of light reflected from the surface of a film, is a useful tool for measuring the thickness and refractive index of thin films [32]. Ellipsometric measurements were carried out using a spectroscopic ellipsometer (Model M-44, J. A. Woollam Company) equipped with a hot stage and a Xe lamp light source. In particular, thickness variations of the nanoscaled films deposited on the Si(100) substrates were measured during stepwise cooling runs from 160 to 25 °C. At each temperature, measurements were taken after the film samples had been held at the temperature for 10 min. The out-of-plane thermal expansion coefficient ($\alpha_\perp$) of a film is defined as follows:

$$\alpha_\perp = \frac{1}{t_0}\left(\frac{\partial t}{\partial T}\right) \quad (1)$$

where the symbols t and T denote the film thickness and temperature respectively, and t_0 is the initial thickness of the film.

3. Results and discussion

3.1. Thermal curing and thermal properties of the films

Fig. 3 shows TGA thermograms of the samples, measured at 2.0 °C/min. As shown in Fig. 3a, during heating up to 130 °C the MSSQ–BTMSE prepolymer undergoes about 7% weight loss, which is probably mainly due to the removal of residual solvent as well as some of the byproducts (water and methanol) of the prepolymer's secondary condensation reaction; above 130 °C weight loss that is mainly due to the further elimination of these byproducts continues very slowly with increasing temperature. This sample shows another significant change in weight above 550 °C, which is attributed to the thermal

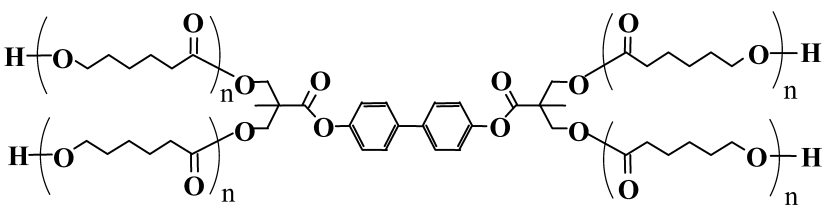

PCL-4

Fig. 2. Chemical structure of the star-shaped poly(ε-caprolactone) porogen, consisting of four arms and a biphenyl core (PCL-4).

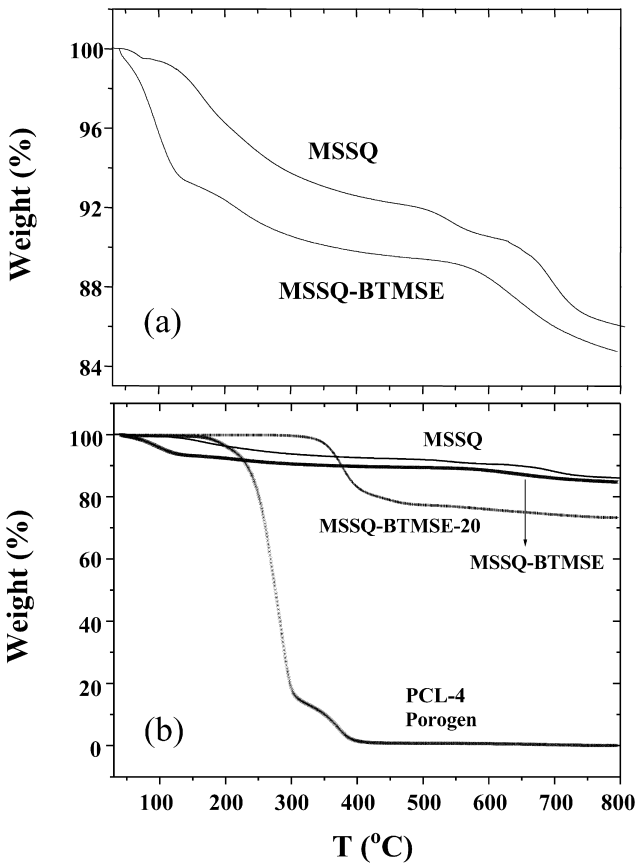

Fig. 3. Thermogravimetric diagrams of MSSQ prepolymer, MSSQ–BTMSE prepolymer, MSSQ–BTMSE-20 composite, and PCL-4 porogen. The MSSQ–BTMSE-20 composite containing 20 wt% PCL-4 porogen was prepared by precuring at 250 °C for 1 h. All thermogravimetric measurements were conducted at 2.0 °C/min under a nitrogen atmosphere.

degradation of cured MSSQ–BTMSE, i.e. of the PMSSQ–BTMSE network. The MSSQ prepolymer does not show any significant weight loss at temperatures below 130 °C, indicating that the amount of residual solvent in the MSSQ sample is relatively low. Above 130 °C the prepolymer exhibits a TGA profile that is similar to that for the MSSQ–BTMSE sample, again due to the evaporation of the byproducts (water and ethanol) of the secondary condensation reaction with increasing temperature. The MSSQ sample exhibits significant weight loss above 500 °C, which is attributed to the thermal degradation of cured MSSQ, i.e. of the PMSSQ network. For both prepolymer samples, the overall weight losses in the range 25–800 °C are 14–15%.

As shown in Fig. 3b, the PCL-4 porogen exhibits a TGA profile which is quite different from those of the MSSQ–BTMSE and the MSSQ samples. The porogen displays a two-step weight loss behavior during heating. In the first step, over the range 170–300 °C, the porogen loses about 87% of its initial weight, which results from thermal degradation of the four arms of the poly(ε-caprolactone); in the second step, over the range 300–400 °C, the sample loses the rest of its weight, because of the thermal degradation of the aromatic core of the porogen.

Fig. 3b also shows a TGA profile of a MSSQ–BTMSE-20 composite (20 wt% porogen initially loaded into 80 wt% MSSQ–BTMSE) that has already been cured at 250 °C for 1 h in vacuum. The weight of the composite sample begins to decrease at around 300 °C and for temperatures up to 500 °C falls in a two-step manner, as was the case for the PCL-4 porogen. The first step is a large weight loss in the range 300–400 °C and the second step is a relatively small weight loss in the range 400–500 °C. The weight losses of both the first and second steps probably result from degradation of the porogen loaded in the composite. Of course, these weight losses are also in part due to the evaporation of the byproducts of the secondary condensation reaction of the MSSQ–BTMSE component, but the contribution of this evaporation is quite small in comparison to that due to the complete calcination of the porogen (see the TGA profiles of the porogen and of the MSSQ–BTMSE sample in Fig. 3b).

However, the degradation temperatures of the porogen in the composite sample are shifted by about 100 °C towards the high temperature region, as seen in Fig. 3b. Taking the TGA profile of the porogen into account, it would be expected that the porogen would degrade partially during precuring at 250 °C for 1 h. However, the weight losses in the range 300–500 °C indicate that the portion of thermal degradation of the porogen in the composite during precuring is relatively small, about 5 wt.% or less with respect to the amount of loaded porogen. This suggests that the porogen becomes more stable in the MSSQ–BTMSE matrix, which may be because of a kinetic barrier to its decomposition produced by the matrix material, and consequently its degradation temperature shifts about 100 °C towards the high temperature region.

In addition, the MSSQ–BTMSE/porogen composites and the MSSQ/porogen composites were cured in vacuum using a two-step protocol, 250 °C/1 h and 420 °C/1 h, and then their TGA thermograms were measured under a nitrogen atmosphere. The cured composites do not reveal any weight loss up to 500 °C, indicating that all loaded porogen is calcined out from the cured matrix polymers in these protocols (data are not shown).

For these TGA measurements, the MSSQ, the MSSQ–BTMSE, and their composites with the PCL-4 porogen were first precured at 250 °C for 1 h in vacuum. Some of the precured samples were further cured at 420 °C for 1 h in vacuum; through this curing process full calcination of the porogen component of the composites took place, generating pores in the composites. The precured and fully cured samples in nanoscaled films (i.e. *nanofilms*) were also examined by ellipsometry and AFM; the results of these measurements are discussed in the following sections.

3.2. Optical and dielectric properties

Figs. 4 and 5 show the refractive indices and dielectric constants of the precured nanofilms as well as of the cured

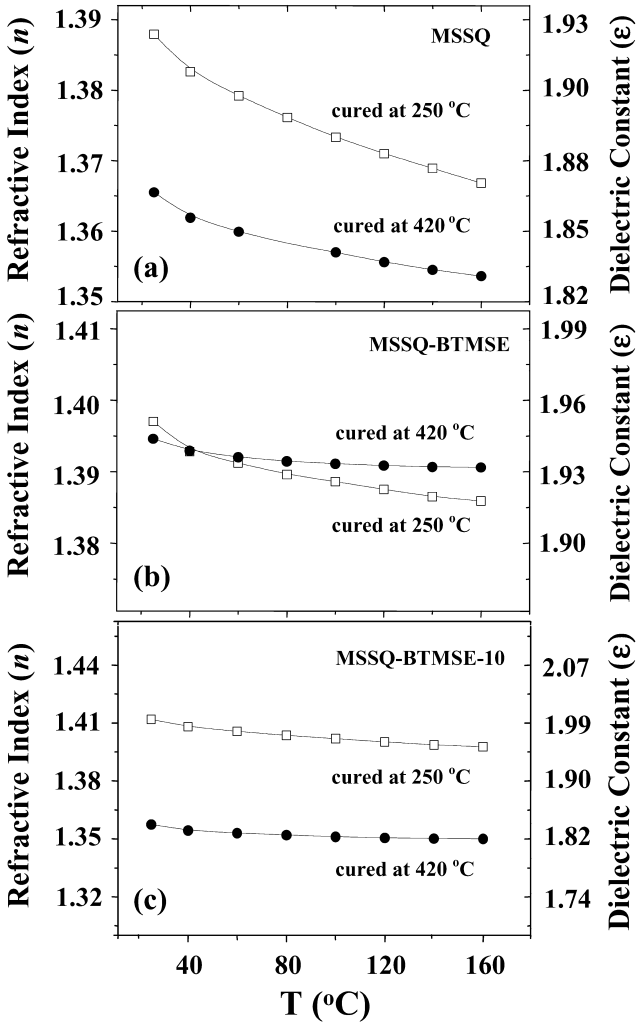

Fig. 4. Ellipsometrically measured refractive indices and dielectric constants of nanoscaled dielectric films cured for 1 h at 250 and 420 °C, and their variations with temperature: (a) MSSQ; (b) MSSQ–BTMSE; (c) MSSQ–BTMSE-10 composite containing 10 wt% PCL-4 porogen.

nanofilms as a function of temperature, as measured by ellipsometry. The data acquisition and ellipsometric modeling procedures used in this work followed the same methods as reported previously [32]. The dielectric constant ε was estimated from the measured refractive index n using the simple Maxwell equation [33]

$$\varepsilon = n^2. \tag{2}$$

The MSSQ film that was cured at 250 °C (i.e. a precured film) exhibits a refractive index of $n = 1.3879$ and a dielectric constant of $\varepsilon = 1.9263$ at 630 nm wavelength at room temperature. The MSSQ film cured at 420 °C (i.e. a fully cured film) exhibits a lower refractive index ($n = 1.3705$) and a lower dielectric constant ($\varepsilon = 1.8783$), compared to the film cured at 250 °C. These differences are probably due to two main factors, chemical composition and density. First, the precured film consists of hydroxyl and ethoxy groups, which have relatively large polarizabilities, in addition to the Si–O silicate linkages and methyl groups

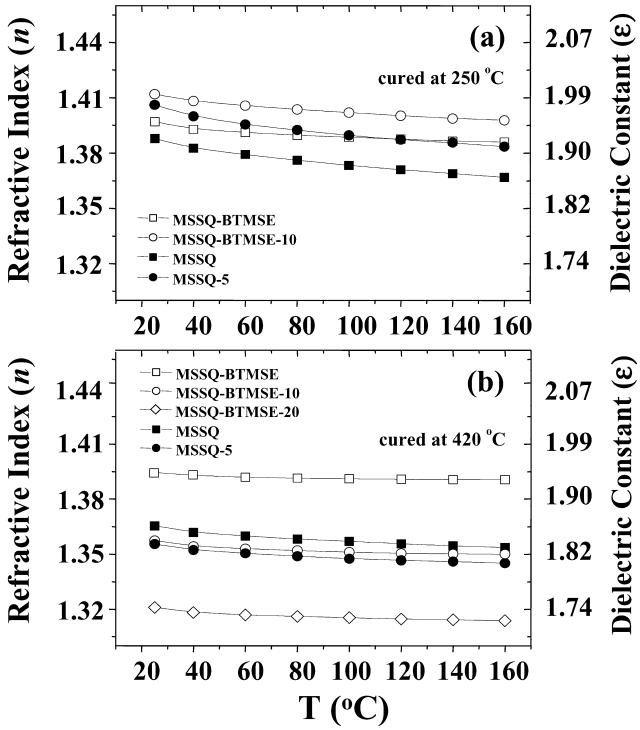

Fig. 5. (a) Ellipsometrically measured refractive indices and dielectric constants of nanoscaled films of MSSQ, MSSQ-5 composite containing 5 wt% PCL-4 porogen, MSSQ–BTMSE, and MSSQ–BTMSE-10 composite containing 10 wt% PCL-4, which were precured at 250 °C for 1 h; (b) ellipsometrically measured refractive indices and dielectric constants of nanoscaled films of MSSQ, porous MSSQ-5, MSSQ–BTMSE, and porous MSSQ–BTMSE-10, which were cured at 420 °C for 1 h.

that are the chemical components of the fully cured film. Second, the precured film might have a higher density than the fully cured film. The refractive index and dielectric constant of the precured film decrease gradually with temperature when heated, as shown in Fig. 4a. The refractive index and dielectric constant of the fully cured film also exhibit a similar temperature dependence to what is observed for the precured film. This temperature dependence might result directly from the thermal expansion of the films that occurs during heating. However, the variation of n (or ε) with temperature has a slightly larger slope in the precured film than in the fully cured film, suggesting that the precured MSSQ film has a larger thermal expansion coefficient than the fully cured film.

On the other hand, the precured and fully cured MSSQ–BTMSE films exhibit $n = 1.3970$ ($\varepsilon = 1.9516$) and $n = 1.3946$ ($\varepsilon = 1.9449$) at 630 nm wavelength, respectively. The refractive index (or dielectric constant) difference between these films is very small. The fully cured MSSQ–BTMSE film exhibits a refractive index very close to that of the precured film although it does not contain hydroxyl and methoxy groups, which have relatively large polarizabilities. This fact suggests that the fully cured MSSQ–BTMSE film is denser than both the precured film and the fully cured MSSQ film (i.e. the PMSSQ film), as shown in Fig. 5.

Regardless of their curing history, the MSSQ–BTMSE films exhibit the n and ε variations with temperature shown in Fig. 4b. These variations with temperature have significantly larger slopes in the precured film than in the fully cured film. These results collectively suggest that the fully cured MSSQ–BTMSE film is denser and less expansive than the precured film.

Fig. 4c shows the refractive indices and dielectric constants of a precured MSSQ–BTMSE-10 composite film and its fully cured film (i.e. its derived porous film). The precured composite film exhibits a refractive index of $n = 1.4120$ ($\varepsilon = 1.9937$), which is larger than that of the precured MSSQ–BTMSE film, as shown in Fig. 5a. The large refractive index (or dielectric constant) of this composite film is due to the relatively large polarizability of the PCL-4 porogen. However, the fully cured film, i.e. the calcined composite film, exhibits a significantly lower refractive index ($n = 1.3574$) and a significantly lower dielectric constant ($\varepsilon = 1.8425$). The reduced n and ε values of the calcined film are due to the pores produced by the calcination of porogen polymer molecules during curing at 420 °C. For both films, the n and ε values are a function of temperature; they decrease slightly with increasing temperature. The variation of n (or ε) with temperature in the fully cured composite film shows a similar trend to that observed for the precured film, but its decay is slightly slower than that of the precured film. Further, the n (or ε) decay with temperature of the porous film is slower than for the precured and fully cured MSSQ films. These results suggest that the fully cured, porous film has slightly less thermal expansivity than either the precured composite film or the fully cured MSSQ film.

As seen in Figs. 4c and 5b, the incorporation of pores via the calcination of porogen molecules into fully cured MSSQ and MSSQ–BTMSE films reduces their refractive indices and dielectric constants. In general, a large increase in the porogen loading in the prepolymer film causes a large reduction in the n and ε of the fully cured film. As seen in Fig. 6, the n and ε of the fully cured film are linearly reduced with increasing porogen loading in the prepolymer composite film.

3.3. Porosity

The relative porosity P of a porous film can be estimated from the refractive indices of the porous film and of the cured matrix using the Lorentz–Lorenz equation [34]:

$$\frac{n_0^2 - 1}{n_0^2 + 2}(1 - P) = \frac{n^2 - 1}{n^2 + 2} \tag{3}$$

where n_0 is the refractive index of the polymer matrix cured at 420 °C and n is the refractive index of the porous composite film prepared at 420 °C.

The estimated porosities are plotted in Fig. 7 as a function of the initial porogen loading. For the MSSQ–BTMSE system, 10 wt% porogen loading produces 8% porosity in the fully cured film, while 20 wt% porogen loading generates 17% porosity. On the other hand, 5 wt% porogen loading creates 4% porosity in the fully cured MSSQ film. These results collectively suggest that the calcination of the PCL-4 porogen molecules during the thermal curing process creates pores in both the MSSQ–BTMSE and MSSQ dielectric matrices.

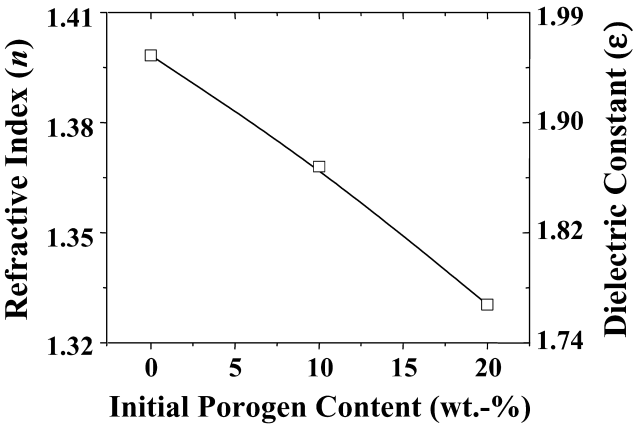

Fig. 6. Variations of refractive index and dielectric constant of porous MSSQ–BTMSE nanofilms as a function of initial porogen loading. Here, the porous dielectric films containing various amounts of PCL-4 porogen were derived from the composite films by cure and calcination at 420 °C for 1 h.

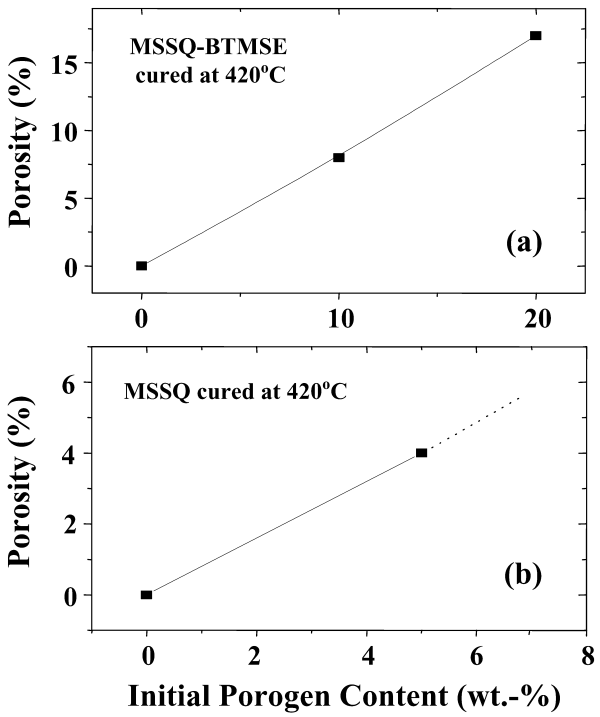

Fig. 7. Porosity variations of porous dielectric films as a function of initial porogen loading: (a) MSSQ–BTMSE; (b) MSSQ. Here, the porous dielectric films containing various amounts of PCL-4 porogen were derived from the composite films by cure and calcination at 420 °C for 1 h.

3.4. Out-of-plane thermal expansivity

The refractive index data described above were measured by ellipsometry. In addition to enabling the measurement of refractive indices, ellipsometry is also a powerful tool for measuring film thickness, particularly for nanoscaled films. Thus, our application of ellipsometry has been extended to the investigation of the thermal expansion behaviors of MSSQ and MSSQ–BTMSE films as well as of their composite films and derived porous films by monitoring film thicknesses during heating and cooling runs as a function of temperature. In these measurements, only the variation of thickness with temperature was monitored, i.e. only out-of-plane thermal expansion was measured.

Fig. 8 shows the measured out-of-plane thermal expansion coefficient ($\alpha_\perp$) data plotted as a function of initial porogen loading. The precured MSSQ–BTMSE film (i.e. precured at 250 °C for 1 h) exhibits $\alpha_\perp = 167$ ppm/°C, while its fully cured film (i.e. cured at 420 °C for 1 h) exhibits $\alpha_\perp = 53$ ppm/°C. On the other hand, for the MSSQ matrix system, $\alpha_\perp$ is 322 ppm/°C for a film precured at 250 °C and 196 ppm/°C for a film fully cured at 420 °C. Regardless of the matrix system, the fully cured films exhibit $\alpha_\perp$ values two or three times smaller than those of precured films. These results confirm the predictions we made above of the thermal expansion behaviors of the MSSQ–BTMSE and MSSQ films on the basis of their refractive index and dielectric constant variations with temperature. The smaller $\alpha_\perp$ values of the fully cured films of a given matrix system probably originate in the more densely networked Si–O linkages in fully cured films, in contrast to the loosely networked structures of the precured films.

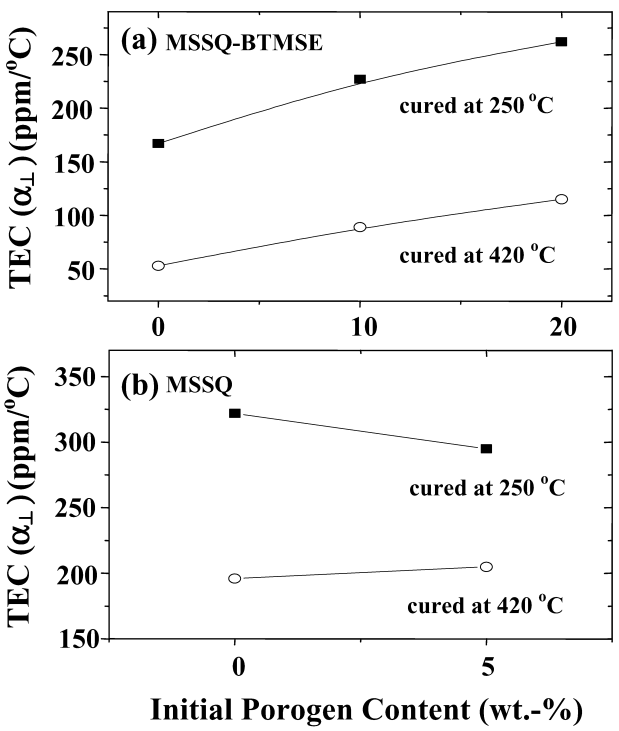

Fig. 8. Out-of-plane thermal expansion coefficient ($\alpha_\perp$) variations of composite dielectric films and their derived porous films as a function of initial porogen loading: (a) MSSQ–BTMSE; (b) MSSQ. Here, composite dielectric films containing various amounts of PCL-4 porogen were precured at 250 °C for 1 h and their porous films derived by cure and calcination of the composite films at 420 °C for 1 h.

The $\alpha_\perp$ of the precured MSSQ–BTMSE film is about two times smaller than that of the MSSQ film precured under the same conditions. Further, the fully cured MSSQ–BTMSE film exhibits an $\alpha_\perp$ almost four times smaller than that of the MSSQ film cured under the same conditions. The MSSQ–BTMSE film always exhibits a smaller $\alpha_\perp$ value than the MSSQ film, regardless of curing history. These smaller $\alpha_\perp$ values of the MSSQ–BTMSE films are probably due to the incorporated BTMSE comonomer units, which chemically bridge two Si atoms. In MSSQ films, all methyl groups are chemically bonded to only a single Si atom, producing defects in the Si–O network structure of the cured film. In contrast, the incorporated BTMSE unit, which is bound chemically to two Si atoms, increases the degree of network formation and also improves the network structure. These two factors are believed to contribute to the observed lower $\alpha_\perp$ values in the MSSQ–BTMSE films. Further, these two factors may cause an increase in film density and consequently increase the refractive index and the dielectric constant of the film. As discussed in an earlier section, the MSSQ–BTMSE film was confirmed as having a larger refractive index and a larger dielectric constant than the MSSQ film.

As seen in Fig. 8a, $\alpha_\perp$ of the precured MSSQ–BTMSE film is altered by the addition of porogen; $\alpha_\perp$ increases as the porogen loading increases. The PCL-4 porogen is a four-armed aliphatic polyester based on a biphenyl core, so its thermal expansivity is expected to be much larger than that of the MSSQ–BTMSE. Thus, the $\alpha_\perp$ increase with increasing porogen loading is due to the high thermal expansivity of the porogen. The porous films derived from the MSSQ–BTMSE/porogen composite films exhibit larger $\alpha_\perp$ values than the fully cured copolymer matrix films. The $\alpha_\perp$ of the porous film increases with increasing initial porogen loading in the composite formation; namely, $\alpha_\perp$ increases with increasing porosity in the film.

Unlike the precured copolymer composite films described above, a precured MSSQ/porogen composite (MSSQ-5) film has a smaller $\alpha_\perp$ value than a MSSQ film precured under the same conditions, as shown in Fig. 8b. These results suggest that MSSQ films precured at 250 °C have slightly larger out-of-plane thermal expansivity than the PCL-4 porogen. However, its porous film (i.e. the calcined film) exhibits a slightly larger $\alpha_\perp$ value than the fully cured MSSQ film, which is due to the pores generated in the film.

3.5. Surface structure

The surface structures of the porous films were examined by atomic force microscopy (AFM). All the porous films exhibited similar AFM images; one of these AFM images is shown in Fig. 9 as a representative surface image, which is that of a porous MSSQ–BTMSE-10 film. As seen in Fig. 9, small islands appear on the film surface. These islands were determined to be about 400 nm in width and 13 nm in height. The islands are distributed at intervals of 1–2 μm on the film surface. These islands are believed to be pores created by calcination during the curing process of the composite film at 420 °C of the PCL-4 porogen molecules which are located just under the film surface. The size of these pores is much larger than the diameter of the star-shaped PCL-4 porogen molecule, estimated under the assumption that its PCL arms are fully extended along the radial direction of the star-shaped porogen. Thus, the observed pore islands might be generated by calcinations of phase-separated porogen aggregates rather than by calcinations of individual single porogen molecules. This suggests that the dimensions of pores made in the dielectric matrix by the calcination of porogen molecules are highly dependent upon the phase-separation pathway of the porogen and matrix polymers and on their resultant aggregate size and distribution. Some research on the microphase separation between matrix materials and porogens has been recently reported in the literature [12,18,35,36]. Such microphase separation may be produced by the migration and aggregation of porogen molecules in the process of drying or/and curing, although film deposition arises from a homogeneous solution in a common solvent. Even though porogen and matrix polymer components are still miscible in the dried film, the crosslink formation processes of the MSSQ or MSSQ–BTMSE matrix components may cause the porogen molecules to phase-separate out from the matrix polymer. In addition, for this porous MSSQ–BTMSE-10 film, no open pores were observed on the film surface. In conclusion, the successful loading of PCL-4 porogen into the MSSQ–BTMSE and the MSSQ matrices produces nanopores that are about 400 nm in diameter by the calcination of these molecules during the curing of the prepolymer matrices.

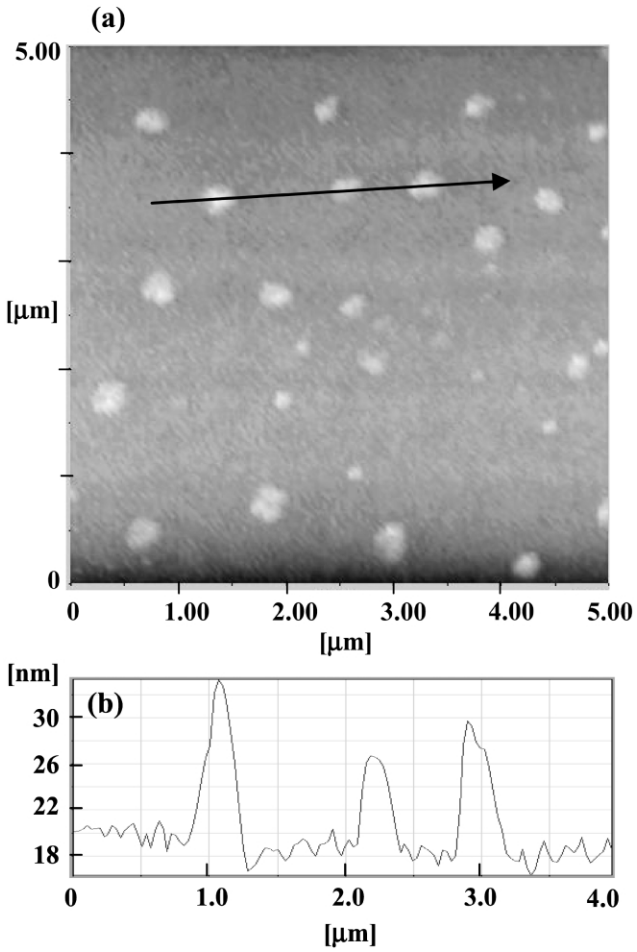

Fig. 9. (a) An atomic force microscopic (AFM) image of a porous nanofilm derived from the MSSQ–BTMSE-10 composite film, containing 10 wt% PCL-4 porogen, by cure and calcination at 420 °C; (b) surface roughness scanned along the arrow line in the AFM image (a). The AFM image was obtained with 5 μm/s scanning speed in non-contact mode.

4. Conclusions

Nanoscaled films of PMSSQ–BTMSE were prepared from soluble MSSQ–BTMSE prepolymer, and their thermal, optical, and dielectric properties were characterized and compared with those of PMSSQ films prepared from soluble MSSQ prepolymer. The curing reactions characteristic of the MSSQ–BTMSE prepolymer were examined by TGA and compared with those of the MSSQ prepolymer.

Even though the copolymer contains only 10 mol% BTMSE comonomer units on the backbone, fully cured MSSQ–BTMSE copolymer (i.e. PMSSQ–BTMSE) is thermally more stable than fully cured MSSQ homopolymer (i.e. PMSSQ); the degradation temperature is 550 °C for the cured copolymer and 500 °C for the cured homopolymer. In addition, the copolymer film always exhibits a larger refractive index and a larger dielectric constant but a smaller out-of-plane thermal expansion coefficient, compared to the homopolymer, when the prepolymers are cured under the same conditions. The contrasting properties of the copolymer result from the chemically bonded ethylenyl linkages between the two Si atoms of the BTMSE comonomer units, which promote a tighter, more perfect network structure in the cured copolymer film.

In addition, composite films of these copolymer and homopolymer dielectrics with PCL-4 porogen were prepared, and their curing reactions and porogen calcinations were investigated by TGA. The thermal, optical, and dielectric properties of the composite films and their derived porous films were examined in detail. Before calcination, it

was confirmed that the presence of the porogen increases the refractive index and the dielectric constant of the copolymer and homopolymer dielectric composite films because of its inherent larger polarizability, and also increases the out-of-plane thermal expansivity of the copolymer composite films, but very slightly decreases the out-of-plane thermal expansivity in the homopolymer composite film. In contrast, it was demonstrated that the star-shaped PCL-4 polymer is a good porogen for the creation of nanopores with diameter on the order of 400 nm during the curing process of the MSSQ–BTMSE and MSSQ prepolymers. It was confirmed that the presence of these nanopores significantly reduces the refractive index and dielectric constant of the porous copolymer and homopolymer dielectric films but increases their out-of-plane thermal expansivity, depending on the initial porogen loading. The porosities of the fully cured copolymer and homopolymer dielectric films containing nanopores were estimated from the measured refractive indices; the surface topographies of the films were also investigated, giving information about the size of the pores generated in the films.

In conclusion, PMSSQ–BTMSE and its nanoporous films on the nanometer scale are candidate materials for use as low and ultra-low dielectric interlayers in the fabrication of advanced microelectronic devices.

Acknowledgements

This study was supported by the Ministry of Industry and Energy and the Ministry of Science and Technology [Korean Collaborative Project for Excellence in Basic System IC Technology (98-B4-C0-00-01-00)] and in part by the Center for Integrated Molecular Systems (KOSEF).

References

[1] Tummala RR, Rymaszewski EJ, editors. Microelectronics packaging handbook. New York: van Nostrand Reinhold; 1989.
[2] Czornyj G, Chen KJ, Prada-Silva G, Arnold A, Souleotis H, Kim S, Ree M, Volksen W, Dawson D, DiPietro R. Proc Elect Comp Tech (IEEE) 1992;42:682.
[3] Lee K-W, Viehbeck A, Walker GF, Cohen S, Zucco P, Chen R, Ree M. J.Adhes Sci Technol 1996;10:807.
[4] Yu J, Ree M, Shin TJ, Wang X, Cai W, Zhou D, Lee K-W. J Polym Sci: Polym Phys 1999;37:2806.
[5] Yu J, Ree M, Park YH, Shin TJ, Cai W, Zhou D, Lee K-W. Macromol Chem Phys 2000;201:491.
[6] Chiang S-K, Lassen CL. Solid State Technol 1999;10:42.
[7] Carter KR. Ultra Low *k* Workshop, ACS Div Polym Chem, Monterey, CA; 14–7 November 1999.
[8] Carter KR, Dawson DJ, DiPietro RA, Hawker J, Hedrick JL, Miller RD, Yoon DY. US Patent No. 5,895,263; 20 April 1999.
[9] Peters L. Semicond Int 1998;September.
[10] Ree M, Goh WH, Kim Y. Polym Bull 1995;35:215.
[11] Hedrick JL, Miller RD, Hawker CJ, Carter KR, Volksen W, Yoon DY, Trollsas M. Adv Mater 1998;10:1049.
[12] Nguyen CV, Carter KR, Hawker CJ, Hedrick JL, Jaffe RL, Miller RD, Remenar JF, Rhee H-W, Rice PM, Toney MF, Trollsas M, Yoon DY. Chem Mater 1999;11:3080.
[13] Oh W, Shin TJ, Ree M, Jin MY, Char K. Macromol Chem Phys 2002; 203:791.
[14] Oh W, Shin TJ, Ree M, Jin MY, Char K. Mol Cryst Liquid Cryst 2001; 371:397.
[15] Cook RF, Liniger EG. J Electrochem Soc 1999;146:4439.
[16] Ying JY, Mehnert CP, Wong MS. Angew Chem Int Ed 1999;38:56.
[17] Nguyen CV, Hawker CJ, Miller RD, Huang E, Hedrick JL, Gauderon R, Hilborn JG. Macromolecules 2000;33:4281.
[18] Lee JK, Char K, Chu SH, Yoon DY. Submitted for publication.
[19] Morgen M, Ryan ET, Zhao J-H, Hu C, Cho T, Ho PS. Annu Rev Mater Sci 2000;30:645. and further references given therein.
[20] Bagley BG, Gallagher PK, Quinn WE, Amos LJ. Proc Mater Res Soc Symp 1984;32:287.
[21] Bolze J, Ree M, Youn HS, Chu SH, Char K. Langmuir 2001;17:6683.
[22] Trollas M, Hedrick JL, Mecerreyes D, Dubois Ph, Jerome R, Ihre H, Hult A. Macromolecules 1997;30:8508.
[23] Ree M, Shin TJ, Park Y-H, Kim SI, Woo SH, Cho CK, Park CE. J Polym Sci: Polym Phys 1998;36:1261.
[24] Ree M, Park Y-H, Kim K, Cho CK, Park CE. Polymer 1997;38:6333.
[25] Ree M, Kim K, Woo SH, Chang H. J Appl Phys 1997;81:698.
[26] Ree M, Nunes TL, Czornyj G, Volksen W. Polymer 1992;33:1228.
[27] Ree M, Chu CW, Goldberg MJ. J Appl Phys 1994;75:1410.
[28] Ree M, Shin TJ, Lee SW. Korean Polym J 2001;9:1.
[29] Ree M, Shin TL, Park YH, Lee H, Chang T. Korean Polym J 1999;7: 370.
[30] Trollsas M, Hedrick JL. J Am Chem Soc 1998;19:4644.
[31] Shin YC, Choi K-Y, Jin MY, Hong S-K, Cho D, Chang T, Ree M. Korean Polym J 2001;9:100.
[32] Oh W, Bolze J, Ree M. Submitted for publication.
[33] Maxwell JC. N Philos Trans 1865;155:459.
[34] Brinker CJ, Scherer CW, editors. Lorentz–Lorenz equation in sol–gel science. San Diego: Academic Press; 1990. p. 803C.
[35] Heise A, Nguyen C, Malek R, Hedrick JL, Frank CW, Miller RD. Macromolecules 2000;33:2346.
[36] Yang S, Mirau PA, Pai C-S, Nalamasu O, Reichmanis E, Lin EK, Lee H-J, Gidley D, Sun J. Chem Mater 2001;13:2762.